

Molybdenum Contamination of Indium, Antimony, Phosphorus Tetramer, and Decaborane Implants

Raymond Pong, and John Schuur

Innovion, 2121 Zanker Road, San Jose, CA, 95131 USA

Abstract. The contamination of indium implants by molybdenum is demonstrated. By extension, molybdenum contamination of antimony, phosphorus tetramer, and decaborane implants are demonstrated. Various mechanisms are identified and demonstrated. Spectrum analysis is confirmed by SIMS. Recommendations for avoidance are presented, both via process and hardware. For the purposes of analysis, one mechanism was deliberately emphasized and yielded 30% contamination of the total implant by molybdenum. The contamination of BF_2^+ implants by the Mo^{++} is well documented. It is anticipated that, since In is used much the same as B from the BF_2^+ implant, the contamination of In by Mo will result in similar device problems.

Keywords: Contamination, Molybdenum

PACS: 85.40.Ry

INTRODUCTION

Indium has been explored as a low diffusivity^{i,ii} replacement for boron. Low solid solubilities make it unsuitable for the formation of shallow source drains and emitters. However, it remains viable for V_T and Base implants.

Multiuse implanters will continue to use BF_3 as a source material for the generation of $^{11}\text{B}^+$ beams. Additionally, some users find the use of AsF_5 attractive.

Fluorinated source gases are well known for their corrosive nature. This leads to high levels of failure in their shutoff valves in comparison to other source gases.

Molybdenum (Mo) has long been used as a refractory metal for the fabrication of the arc chambers for the generation and containment of source plasmas. It has long been known to result in the contamination of $^{49}(\text{BF}_2)^+$ beams with doubly charged Mo (Mo^{++}).

Source plasma complexes were previously demonstrated in the formation of $^{31}(\text{BFH})^+$, resulting in the aliasing for $^{31}\text{P}^+$.ⁱⁱⁱ

This paper will demonstrate the failure modes for the contamination of $^{115}\text{In}^+$ beams with Mo and recommend actions to prevent or minimize this contamination.

EXPERIMENTAL DESIGN

An Axcelis GSD200 is used to generate the various beams under study. The system uses molybdenum arc chamber to generate and contain the source plasmas. In particular, CO_2 , N_2 , Ar, and BF_3 are used as source gases to generate the $^{16}\text{O}^+$, $^{14}\text{N}^+$, $^{40}\text{Ar}^+$, and $^{19}\text{F}^+$ plasmas. An indium vaporizer is used to generate the $^{115}\text{In}^+$ beams. The other gases are introduced into the indium plasma as carrier gases in order to simulate gas leaks. The spectrum function of the GSD operating system is used to capture peak heights of the various constituents of the source plasmas under study. SIMS analysis is used to demonstrate the existence of the MoF and MoO species in the In source plasmas with simulated BF_3 leaks.

EXPERIMENTAL RESULTS AND DISCUSSION

The spectrum of an indium source plasma is shown in Figure 1. The vaporizer temperature is set at a low value to limit the beam current for low dose applications. Argon is used to supply the electrons for the plasma.

Figure 2 is the same spectrum as in Figure 1. This is plotted with a logarithmic y scale to better highlight

the smaller peaks. Note that the shoulder for the ^{113}In is clearly identifiable in this format.

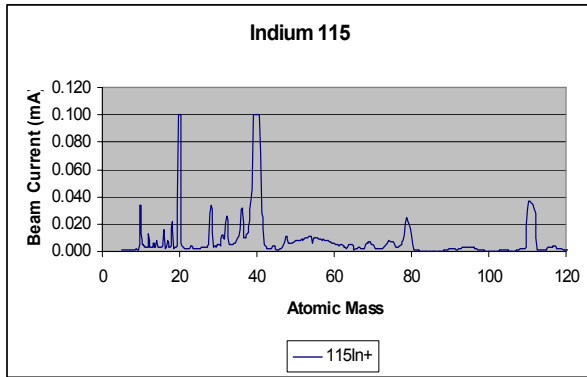


Figure 1 – Argon used to supply the secondary electrons for the In source.

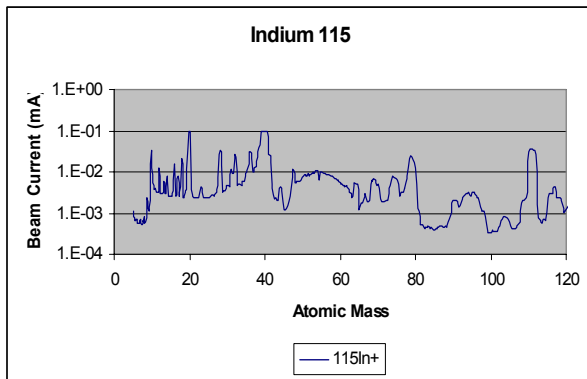


Figure 2 – The same spectrum but with beam current scaled logarithmically.

A test wafer with a dose of $4e13$ was implanted with the beam in Figure 2. The SIMS analysis of that

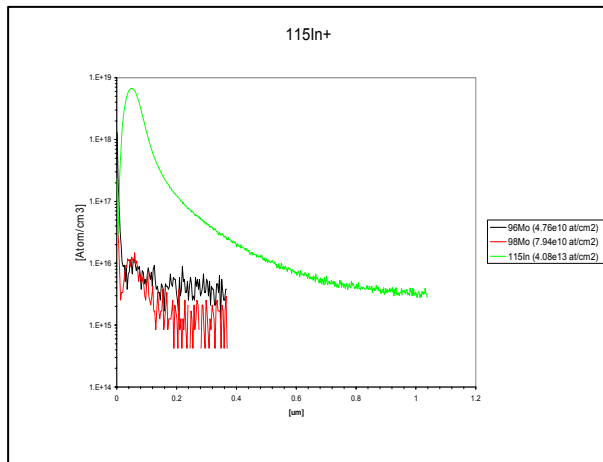


Figure 3 – SIMS analysis of beam from figure 2 at dose of $4e13$. Note ^{96}Mo and ^{98}Mo at detection limits.

wafer is shown in Figure 3. The wafer was analyzed for the presence of ^{96}Mo and ^{98}Mo . Both of these isotopes are at the detection limit for this analysis.

This same source plasma is now used with BF_3 replacing the argon. The spectrum from this plasma is in Figure 4. A shoulder is clearly visible at the location expected for ^{113}In . A reasonable but erroneous assignment would be that is from the ^{113}In isotope.

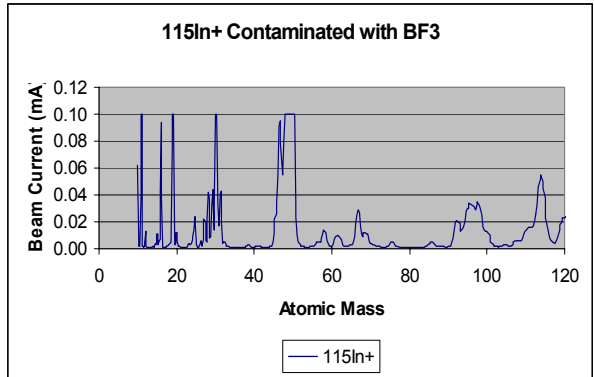


Figure 4 – Low current indium beam using BF_3 to supply the secondary electrons. Note the shoulder at the location of the ^{113}In .

A test wafer with a dose of $4e13$ is created and analyzed with SIMS. This analysis is shown in Figure 5. Note that the ^{96}Mo dose is roughly half of the ^{115}In dose. The F concentration profile closely follows that of the ^{115}In profile. This clearly demonstrates that 30% of the beam is composed of $^{96}\text{MoF}^+$. Additionally 3% of the sample is ^{98}Mo . This indicates

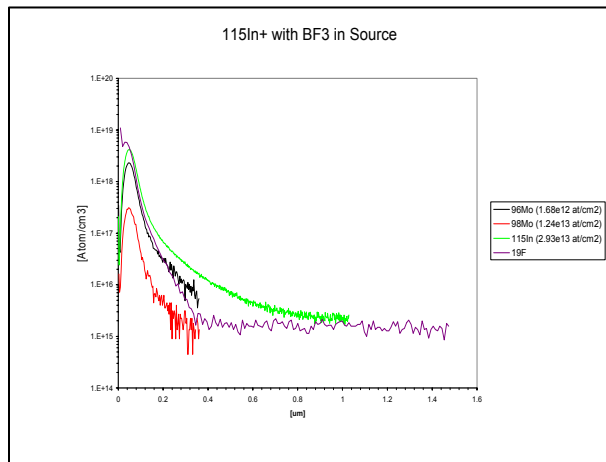


Figure 5 – The ion beam from figure 3 above to a dose of $4e13$. Note the presence of F at approximately the same concentrations as the ^{96}Mo .

that the complex being implanted for this is the $^{96}\text{MoO}^+$ species at mass 114 as opposed to the $^{98}\text{MoF}^+$ at 117AMU. Poor mass resolution in the GSD series of implanters at these high AMU values results in the MoO peak being wide enough to be part of the AMU 115 peak. In this instance, due to the analytical technique it was not possible to measure the O concentrations as was done for the F.

A spectrum of an argon source plasma with the Indium vaporizer turned off is shown in Figure 6. This clearly shows that there are no peaks in the AMU115 region that have the characteristic pattern of the Mo isotopes. Therefore, aside from 1) be a noble gas that does not bond to other atoms and 2) any complexes would be much higher in AMU, the spectrum indicates that there are no argon complexes to alias with the $^{115}\text{In}^+$ beam. Clearly the Mo isotopes are in the source plasma. Therefore these are sputtered from the arc chamber walls.

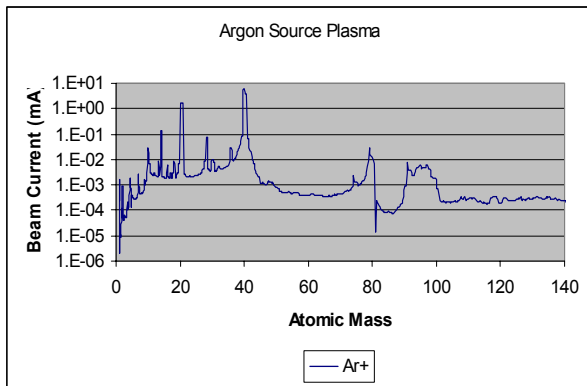


Figure 6 – Spectrum of an argon source plasma. Note the Mo isotopes.

A spectrum of a BF_3 source is shown in Figure 7. One can see the characteristic distribution of Mo isotope peaks around the AMU115 regime. This indicates the presence of the MoF isotope peaks. This

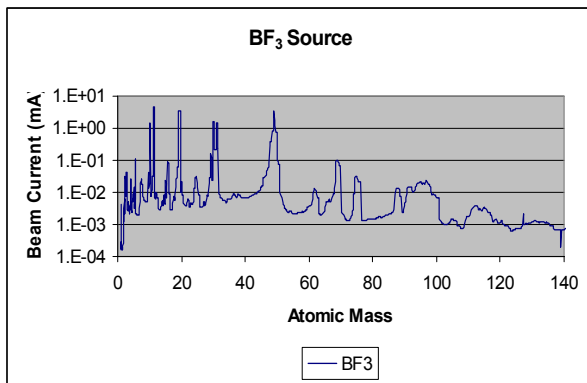


Figure 7 – Spectrum of BF_3 source plasma extended to 140AMU. Mo isotopes clearly delineated.

supports the SIMS analysis that shows the presence of ^{96}MoF . Though it not readily identifiable in this spectrum, MoF_2^+ isotope peaks are visible in other spectrums.

Figure 8 shows a spectrum of a source plasma using CO_2 as the source gas. The characteristic peak distributions of the Mo isotopes are clearly identifiable. Also identifiable are the replication of those peak distributions offset by +16AMU, +32AMU, and +48AMU. This indicates the presence of the MoO^+ , MoO_2^+ , and MoO_3^+ ion species. The strength of these peaks supports the conclusion previously drawn that the presence of the $^{98}\text{Mo}^+$ isotope in the $^{115}\text{In}^+$ sample is due to the formation of MoO. The strength of the complexing between Mo and O suggests that this MoO will exist even with only small levels of O in the source plasma. It has been previously demonstrated that F^+ from fluorinated source gases such as BF_3 , will displace O from the Al_2O_3 insulators to create the AlF volatile species as the precursor for the generation of Al+ beams.^{iv} This reaction is hypothesized to release the O^+ into the source plasma that then complexes with the Mo isotopes to form the MoO species when there is a BF_3 source plasma.

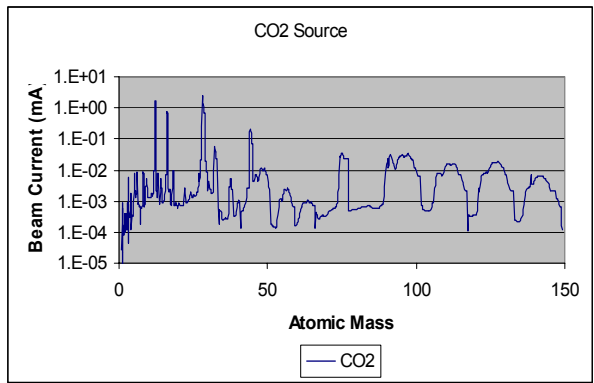


Figure 8 – Spectrum of CO_2 source plasma extended to 150AMU. Demonstrates the existence of MoO^+ , MoO_2^+ , and MoO_3^+ .

Figure 9 shows the spectrum of a plasma created with N_2 . Again, the characteristic isotope distribution and natural abundance is clearly seen for Mo. In this case, we also see the same distribution offset by +14AMU, indicating the presence of the MoN^+ complexes. Less clear but highly suggestive are the peak distributions at 118 to 128. These may indicate the presence of MoN_2^+ complexes.

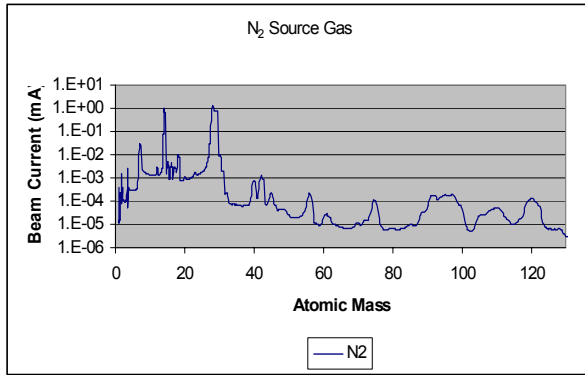


Figure 9 – Spectrum of N₂ source plasma extended to 130AMU. Demonstrates the existence of MoN⁺ and suggests the existence of MoN₂⁺.

Given the possibility for the creation of these Mo complexes, it is clear that in the implantation of ¹¹⁵In⁺ and other high mass species for low dose applications, one must either use arc chambers that do not contain Mo or be very diligent to insure that no leaks exist in the source. It is often assumed that because the analyzer is a very good tool to separate out masses, that it will also serve to insure that there is no atomic contamination. In general this is true but one must be alert for the possibility of molecular aliasing.

Molybdenum Ion Complex	Mass Range in AMU	Ion Species Affected
MoN ⁺	104 – 114	B ₁₀ ⁺
MoN ₂ ⁺	118 – 128	Sb ⁺ , P ₄ ⁺
MoO ⁺	106 – 116	B ₁₀ ⁺ , In ⁺
MoO ₂ ⁺	122 – 132	Sb ⁺ , P ₄ ⁺
MoF ⁺	109 – 119	In ⁺
MoF ₂ ⁺	128 – 138	

REFERENCES

- ⁱ A.S. Grove, Physics and Technology of Semiconductor Devices, John Wiley and Sons, Inc., New York, ©1967
- ⁱⁱ S.M. Sze, Physics of Semiconductor Devices, 2nd Edition, John Wiley & Sons, New York, ©1981
- ⁱⁱⁱ R. Pong, C. Heden, W. Weisenberger, “The Contamination of Phosphorus Implants with BFH”, Spring 1996 meeting of the Electrochemical Society.
- ^{iv} R. Pong, W. Weisenberger, “A Displacement Reaction Source for the Generation of Al⁺”, IIT Kyoto.